Unsteady flows in a compound open-channel: a laboratory experiment and a 1D+ model

Y. Kaddi, Sébastien Proust, J.B. Faure, F.X. Cierco

▶ **To cite this version:**

Y. Kaddi, Sébastien Proust, J.B. Faure, F.X. Cierco. Unsteady flows in a compound open-channel: a laboratory experiment and a 1D+ model. 38th IAHR World Congress, Sep 2019, Panama City, Panama. pp.2839-2848. hal-02609740

HAL Id: hal-02609740
https://hal.inrae.fr/hal-02609740

Submitted on 16 May 2020

HAL is a multi-disciplinary open access archive for the deposit and dissemination of scientific research documents, whether they are published or not. The documents may come from teaching and research institutions in France or abroad, or from public or private research centers.

L'archive ouverte pluridisciplinaire **HAL**, est destinée au dépôt et à la diffusion de documents scientifiques de niveau recherche, publiés ou non, émanant des établissements d'enseignement et de recherche français ou étrangers, des laboratoires publics ou privés.

UNSTEADY FLOWS IN A COMPOUND OPEN-CHANNEL: A LABORATORY EXPERIMENT AND A 1D+ MODEL

YASSINE KADDI(1), SÉBASTIEN PROUST(2), JEAN-BAPTISTE FAURE(3) & FRANÇOIS-XAVIER CIERCO(4)

(1,2,3) Irstea-Lyon, Villeurbanne, France
yassine.kaddi@irstea.fr; sebastien.proust@irstea.fr; jean-baptiste.faure@irstea.fr
(4) CNR , Lyon, France,
F.CIERCO@cnr.tm.fr

ABSTRACT

This paper investigates the physical and numerical modellings of unsteady overbank flows in a compound open-channel, which consists in a main channel (MC) and one adjacent floodplain (FP). The experiments were performed in an 18 m long and 2 m wide flume. Simulations using the 1D code MAGE coupled with an improved one-dimensional (denoted as 1D+) method termed ISM (Independent Subsections Method, Proust et al. 2009) are compared to the experimental data. The originality of the ISM lies in its solving of the momentum conservation equation in each of the channel sub-sections (MC and FP). The ISM explicitly models the depth-averaged Reynolds stress at the MC/FP interface, and the transverse exchanges of mass and momentum by the mean flow between MC and FP. It also accounts for the upstream discharge distribution between MC and FP. As this method has been validated only for steady non-uniform flows, the present study aims at validating it under unsteady flow conditions. Hydrographs are injected at the flume entrance in the MC and FP, with 100 runs in order to compute ensemble averages of the flow parameters. The ratio of FP discharge to total discharge equals to 7 % at baseflow and 15 % at peakflow, while the ratio of FP flow depth to MC flow depth ranges from 0.14 to 0.30. It was found that the ISM could accurately predict the temporal variations in: (i) the flow depth along the flume; (ii) the depth-averaged streamwise and transverse velocities at the MC/FP interface; and subsequently (iii) the interfacial lateral discharge per unit length.

Keywords: Unsteady flow, compound open-channel, laboratory experiment, improved one-dimensional model

1 INTRODUCTION

River floods can give rise to overbank flows that are often represented as flows in a compound channel, which consists in the river main channel (MC) and one or two adjacent floodplains (FPs). The physics of overbank flows is complex owing to the combined effects on the flow structure of: (i) planform large-scale vortices forming at the interface between MC and FP; and (ii) the lateral transfers of mass and momentum by the time-averaged flow between MC and FP when flow is non-uniform in the streamwise direction. The planform large-scale vortices were first explored by Sellin (1964) for streamwise uniform flows. The conditions of emergence of these Kelvin-Helmholtz-type coherent structures were investigated by Proust et al. (2017) and Proust and Nikora (2018) for both uniform and non-uniform flows. The lateral transfers of mass and momentum by the time-averaged flow under steady non-uniform flow conditions have been extensively investigated in laboratory flumes (e.g., Eliott and Sellin (1991), Bousmar et al (2004), Proust et al. (2006), Proust et al. (2013), Peltier et al. (2013a), Dupuis et al. (2017b), Proust et al. (2017)).

Unsteady compound channel flows have been far less experimentally studied. They were explored by Tominaga et al. (1995) in a compound channel with two symmetrical FPs. These authors observed that the peak velocity preceded the peak water level, similarly to what was observed in a single rectangular channel, but with a time lag between the two peaks higher in a compound channel than in

a single channel. Lai et al. (2000) studied the flood-wave propagation in a compound open-channel by injecting at the flume entrance hydrographs with a variable duration. The longitudinal changes in the hydrograph shape, the front wave propagation and flow depth – velocity relationships were investigated. It was e.g. found that the flood wave decreases exponentially along the channel for the shorter hydrographs.

In addition to analyzing the longitudinal propagation of a hydrograph, the present study firstly aims at experimentally investigating the time-varying depth-averaged lateral exchange of streamwise momentum by the mean flow at the vertical interface between MC and FP (Reynolds shear stress are not analyzed here). The second purpose of the study is to validate an improved one-dimensional (denoted as 1D+) method, termed Independent Subsections Method (ISM, Proust et al. 2009), under unsteady flow conditions. Indeed, this method has been validated so far only for steady uniform (Bousmar et al. 2016) and non-uniform flows in compound open-channels (Proust et al. 2009, Proust et al. 2010) and for various land uses of the FPs (Proust et al. 2016). Unlike classical 1D approach (Nicollet and Uan 1979, Bousmar et al 1999) that solves the dynamic equation (Saint-Venant or Bernoulli) on the total cross-section, the ISM solves it in each subsection (MC, right-hand or left-hand FPs), resulting in a system of 4 coupled equations. Under steady flow conditions, the ISM captures a better physics linked to overbank flows, notably the mass and momentum exchanges between MC and FPs, and eventually, simulate more accurately both flow depth and velocity in the FPs (Proust et al, 2009). One remaining key issue is: is it worth using this 1D+ method in the presence of transient flows?

The paper outlines the experiments in section 2 followed by the experimental results in section 3. The 1D+ model is then introduced in section 4 before comparing the 1D+ simulations and the experimental data in section 5. Conclusions are eventually drawn in section 6.

2 LABORATORY EXPERIMENT

2.1 Flume and measuring devices

The experiments were conducted in an 18 m long and 2 m wide compound open-channel flume (Figure 1) in the Hydraulics and Hydro-morphology Laboratory at Irstea Lyon-Villeurbanne, France. The longitudinal bed slope was $S_o = 1.05 \times 10^{-3}$. The compound cross-section consisted in a 1 m wide rectangular glassed-wall MC and in a 1 m wide adjacent FP covered by dense synthetic grass (5 mm high rigid blades). The Manning roughness coefficients over the FP, n_f, and in the MC, n_m, were 0.0114 $m^{-1/3}$.s and 0.0096 $m^{-1/3}$.s respectively.

The vertical distance from the MC glass bed to the blades top was 0.117 m, defining the bank-full stage in the MC. The MC and the FP are supplied with water by two independent inlet tanks. Each sub-section flow rate (Q_m in the MC and Q_f in the FP) is monitored with dedicated electromagnetic flow-meters (Waterflux) at an acquisition rate of 50 Hz. Independent hydrographs can be injected at the flume entrance in the MC and FP. A Cartesian right-handed coordinate was used in which X-, Y-, and Z-axes are aligned with the longitudinal (parallel to flume bottom), transverse, and vertical (normal to flume bottom) directions. The origin is defined as: X = 0 at the outlet of the two inlet tanks; Y = 0 at the side-wall of the MC; and Z = 0 at the MC glass bed.

Water surface elevations were measured with six ultrasonic sensors (BAUMER UNDK 20I6912/S35A) located in MC and FP at longitudinal positions X = 6 m, 7 m, 10 m, 13 m, 14 m and 15 m (Figure 1). At each measuring point, elevation is recorded at a rate of 50 Hz with an accuracy better than 0.3 mm. Velocities were measured at the interface between MC and FP at several altitudes over the water column at X = 10 m, using a side-looking ADV probe (Vectrino Plus, Nortek) with a sampling rate of 100 Hz and an accuracy of 0.5% of the measured velocity.

2.2 Flow conditions

In order to find the time-varying mean flow parameters (water elevation and velocity), the ensemble-averaging method is used. One hundred symmetric hydrographs are injected at the flume entrance. Each hydrograph is composed of a steady base flow (discharge Q^b), a linear rising limb until the peak flow (discharge Q^p), and of a linear falling limb. The associated unsteadiness flow parameter λ (Eq. 1, where T_r is the rising limb duration) equals to 0.26 in MC and 0.46 in FP (same order of magnitude of the λ-values of Chan-ji et al. (2000)). The parameter λ represents the ratio of the water surface rising speed to the wave speed at the peak flow.

$$\lambda = \frac{<h^p> - <h^b>}{S_o T_r \sqrt{g <h^p>}} \quad (1)$$

where $<h^p>$ and $<h^b>$ are the ensemble averages of flow depth at peak flow and base flow respectively.

The flow parameters of the base flow and peak flow are reported in Table 1, where Q is total discharge (sum of the MC and FP discharges, $Q_m + Q_f$), h_m and h_f are flow depths in MC and FP respectively, $h_r = h_f / h_m$ is the relative flow depth. The unsteadiness parameters in MC and FP, λ_m and λ_f, are also given. It should be noted that all the values reported in Table 1 are ensemble averages over the 100 hydrographs. In addition, the values of h_m and h_f for the base and peak flows correspond to averages of the measured values at the six X-positions in a sub-section.

2.3 Data treatment

Both instantaneous values of water level and velocity were filtered. The ADV velocity data are filtered based on the values of signal to noise ratio (SNR) and signal correlation (COR). The velocity data with a SNR lower than 22 dB and a COR lower than 85% were removed from the time series. To account for a likely small misalignment of the ADV probe with the longitudinal direction, a correction of the transverse velocity data was carried out following Peltier et al. (2013b).

To perform ensemble averages of water depth and velocity, a windowing of instantaneous data was carried out by (1) detecting the peak discharge value of $Q_m(t)$ or $Q_f(t)$ and (2) considering a window centered on the peak value. The window width was chosen to include the baseflow before and after one hydrograph, and the rising and falling limbs. An ensemble average of each instantaneous flow parameter P(t) was then computed using the 100 hydrographs. The ensemble average $<P>(t)$ and the associated standard deviation σ_P (t) are defined in Eqs. 2 and 3 respectively.

$$< P > (t) = \frac{1}{100} \sum_{i=1}^{100} P_i(t) \quad (2)$$

$$\sigma_P(t) = \sqrt{\frac{1}{100} \sum_{i=1}^{100} (P_i(t) - < P(t) >)^2} \quad (3)$$

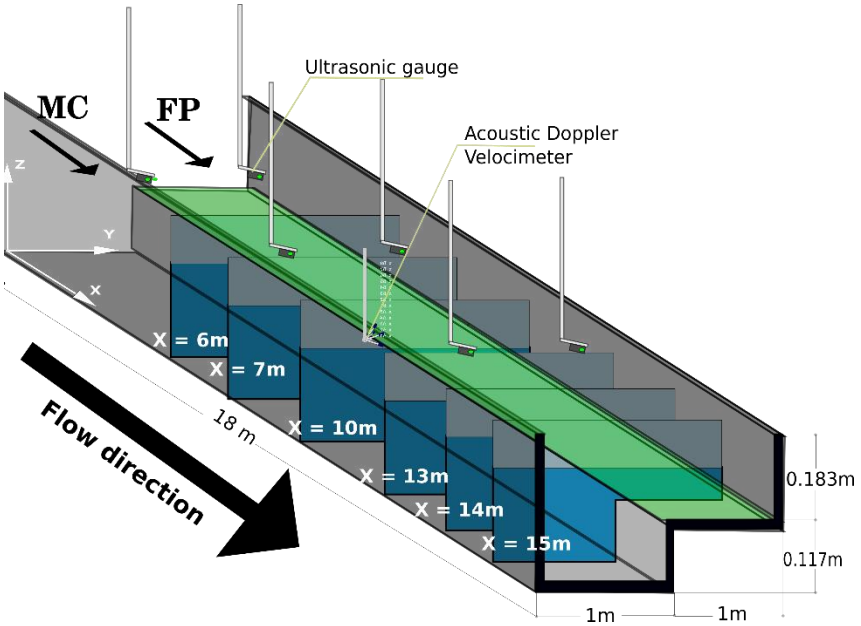

Figure 1: Sketch of the compound open-channel flume with a glassed-wall main channel (MC) and a floodplain (FP) covered by dense synthetic grass

Table 1: Flow parameters of the base flow and peak flow (ensemble averages based on the 100 hydrographs).

	Q_m	Q_f	Q	Q_f/Q	$\langle h_m \rangle$	$\langle h_f \rangle$	$\langle h_r \rangle$	λ_m	λ_f	T_r
	Ls^{-1}	Ls^{-1}	Ls^{-1}	%	mm	mm				s
Baseflow	94	7	101	7	136	20	0.14			
								0.26	0.46	90
Peak flow	142	26	168	15	166	50	0.30			

3 EXPERIMENTAL RESULTS

3.1 Inlet Hydrographs

Figure 2 shows the ensemble-average of the total inlet discharge $\langle Q \rangle(t)$ (with $\langle Q \rangle(t) = \langle Q_m \rangle(t) + \langle Q_f \rangle(t)$) and the standard deviation σ_Q (t) as a function of time. The values of σ_Q are higher during the rising and falling limbs than during the baseflow. First, this is due to the windowing technique (section 2) that is applied to each hydrograph, which can lead to a small time shift between two hydrographs. Second, the repeatability of Q(t) may be weaker for a transient flow than for the steady base flow. Last, the σ_Q - value is lower at peak flow than during the rising and the falling limbs as windowing is centered on the peak value of Q(t). A convergence test (not shown here) indicates that the ensemble-averaged discharge values stabilized between ± 0.2 Ls^{-1} after 60 runs in FP and MC.

3.2 Stage hydrographs

Figure 2 also shows the ensemble-averaged FP flow depth $\langle h_f \rangle$ (t) at X= 6 m. As observed for Q(t), the values of standard deviation σ_{hf} are higher during the rising and falling limbs than at the peak flow and during the base flow. A similar result is obtained for MC flow depth $\langle h_m \rangle$(t) (not shown here). Note that the flow depth standard deviation values are of the same order of magnitude as the fluctuations of the instantaneous flow depth (~ 4 mm).

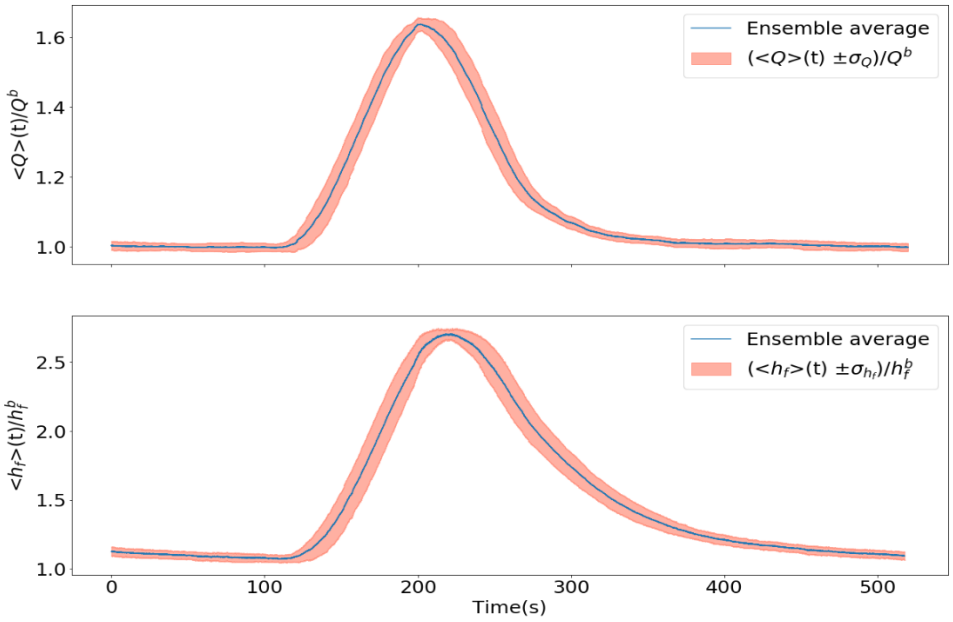

Figure 2: Inlet total discharge normalized by the baseflow total discharge (top). Water depth in the FP normalized by the baseflow FP water depth at X = 6 m (bottom).

The convergence of FP flow depth with the number 'i' of hydrographs is displayed in Figure 3. The difference $<h_{fi}>$- $<h_f>$ is plotted with respect to number 'i', where $<h_{fi}>$ is calculated based on a number i of runs and $<h_f>$ is computed with 100 runs. The read area represents the ultrasonic probe accuracy (±0.3mm). The same result is obtained for $<h_m>$ (not shown here). The water depths $<h_m>$ and $<h_f>$ are converged after 90 runs.

The water depths at various X-positions are plotted in Figure 4. Water depth is normalized by the baseflow water depth, denoted as h_m^b in MC and h_f^b in FP. Time is normalized by T_p = duration of base flow + T_r. The wave subsidence is not similar in MC and FP, which was not observed by Chan-ji et al. (2000). This can be explained by the fact that in the present experiments, two independent hydrographs are simultaneously injected in MC and FP. This results in two different wave propagations (and wave velocities) in both subsections, while in Chan et al. (2000), only the MC was supplied with water at the flume entrance, the overflow over the FPs occurring during the rising limb.

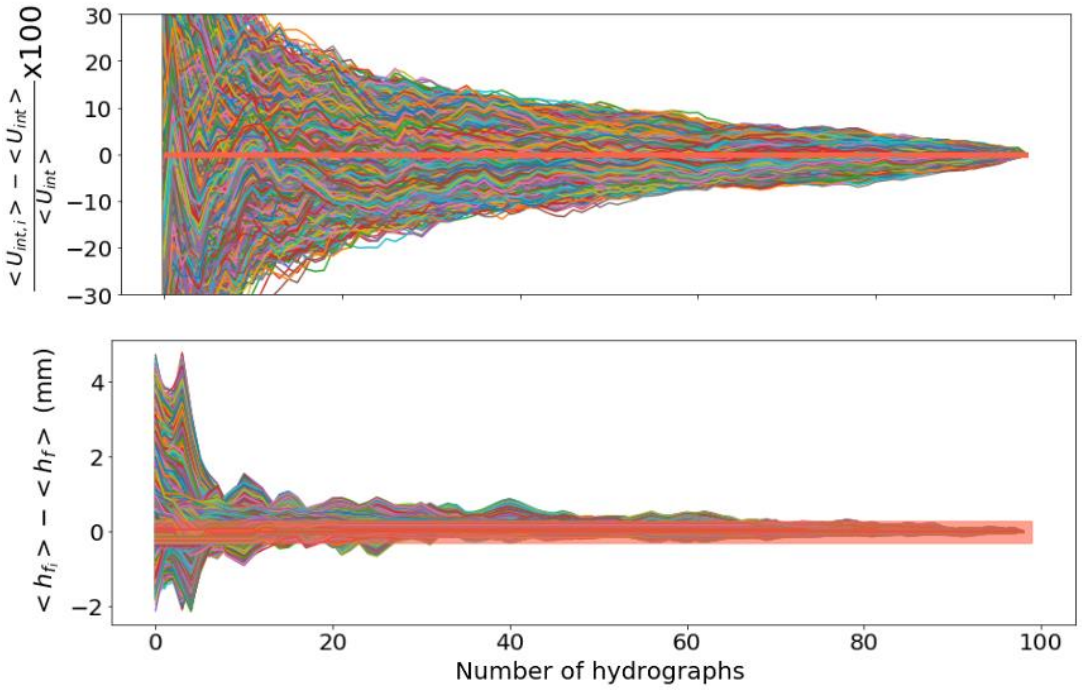

Figure 3: Convergence tests for the measured interfacial velocity at X = 10 m (top) and for the measured FP flow depth at X = 6 m (bottom). The red area represents the probes accuracy.

3.3 Interfacial velocity

The time-varying velocity at the MC-FP interface was measured at eight various elevations. At each elevation, velocity data were recorded for the 100 runs. The depth-averaged time-varying velocity was then computed. We will present in the sequel the depth-averaged streamwise velocity $<U_{int}>_d$, transverse velocity $<V_{int}>_d$, and the lateral discharge from FP to MC per unit length q.

The convergence of the interfacial velocity is illustrated in Figure 3. The difference $<U_{int,i}>$ - $<U_{int}>$ is plotted against the number 'i' of hydrographs, where $<U_{int,i}>$ is calculated based on a number i of runs and $<U_{int}>$ is computed with the 100 runs. The measurements were taken 9 mm above the FP bottom. Because of the high fluctuations of velocity at the interface, where the core of the planform shear layer turbulence is located, the U_{int} value reached ± 2% of the ensemble-averaged velocity, which is higher than the ADV's accuracy, i.e. 0.5% of the measured velocity (red area in Figure 3). As the convergence was not perfect, we also used a moving average method to smoothen the depth-averaged value $<U_{int}>_d$.

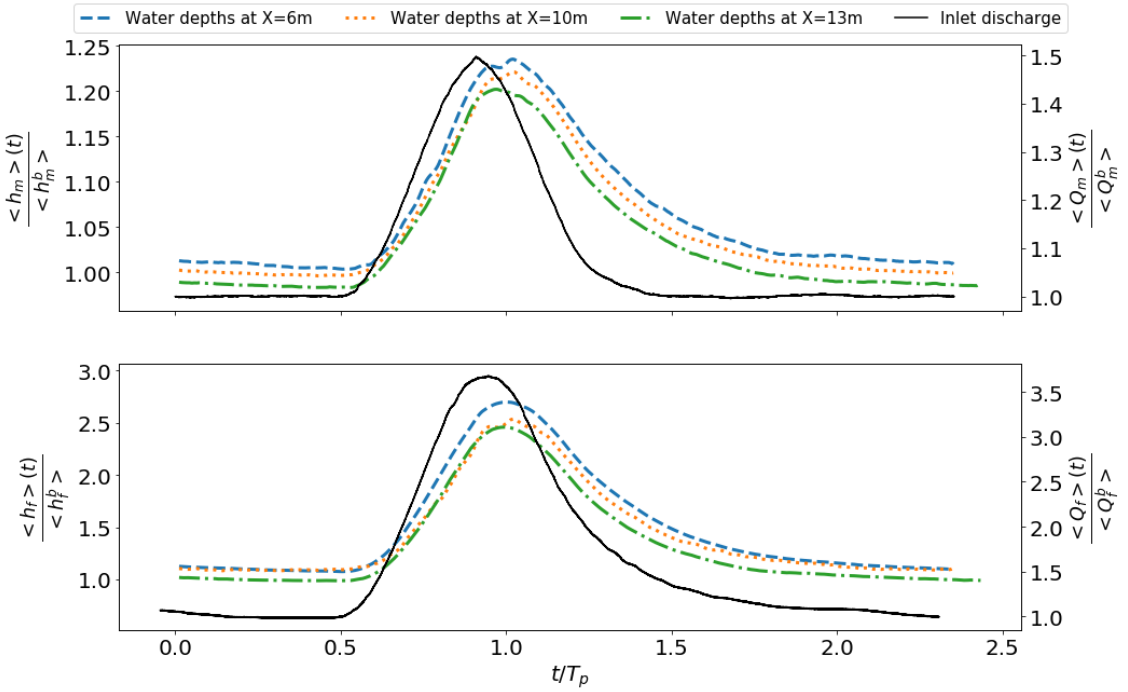

Figure 4: Water depth measured in MC (top) and FP (bottom) at various X-positions, and inlet discharges in MC and FP (measured by the flowmeters upstream of the two inlet tanks).

4 1D+ MODELLING

The previous experiments were simulated using a 1D+ method that is termed ISM (Independent Sub-sections Method, Proust et al. 2009) and is implemented in the 1D code Mage (developed at Irstea). The originality of the ISM lies in its solving of the momentum conservation equation in each of the channel sub-sections (MC and FP), which enables the subsection head loss slopes to be different in MC and FP. The ISM explicitly models the depth-averaged Reynolds shear stress and the mass and momentum exchanges by the mean flow between MC and FP. In addition, it accounts for the actual (measured) upstream discharges in MC and FP, Q_m and Q_f.

4.1 Mass and momentum conservation equations

In the case of a compound open-channel consisting in one MC and two adjacent FPs, the ISM is a system of four coupled differential equations (one mass conservation equation on the total cross-section, and three momentum conservation equations (one per subsection)). Here, with only one FP, the system is composed of three equations as follows:

$$\frac{\partial A}{\partial t} + \frac{\partial (Q_m + Q_f)}{\partial x} = 0 \tag{4}$$

$$\frac{\partial Q_m}{\partial t} + \frac{\partial}{\partial x}\left(\frac{Q_m^2}{S_m}\right) + gA_m \frac{\partial Z}{\partial x} = -gA_m J_m - \frac{\tau_{int} h_f}{\rho} + U_{int} q \tag{5}$$

$$\frac{\partial Q_f}{\partial t} + \frac{\partial}{\partial x}\left(\frac{Q_f^2}{S_f}\right) + gA_f \frac{\partial Z}{\partial x} = -gA_f J_f + \frac{\tau_{int} h_f}{\rho} - U_{int} q \tag{6}$$

where A is total wetted area, Z is water surface elevation with respect to a reference datum, q is the lateral discharge per unit length (positive with a flow from MC to FP) defined in Eq. 7, A_i is subsection area, J_i is subsection head loss gradient, h_i is subsection flow depth with i = m or f in MC and FP respectively, U_{int} and τ_{int} are the depth-averaged mean streamwise velocity and transverse Reynolds shear stress at the MC/FP interface, respectively.

$$q = \frac{\partial A_f}{\partial t} + \frac{\partial Q_f}{\partial x} \quad (7)$$

4.2 Closure equations at the interface

First, we can assume that interfacial streamwise velocity equals to the subsection-averaged velocity in the subsection i ($U_{int} = U_i$) when a lateral mean flow occurs from subsection i to subsection j. This assumption was applied e.g., in Proust et al. (2016) for flows subject to a longitudinal change in FP land use. Second, we can consider velocity U_{int} as a function of the subsection-averaged velocities U_m and U_f, like in the case of non-prismatic channels (Proust et al. 2010). We used the latter assumption here:

$$U_{int} = \phi U_m + (1 - \phi) U_f \quad (8)$$

where ϕ = weighting coefficient.

To model the interfacial Reynolds shear stress τ_{int} related to the turbulent exchange by the horizontal large-scale Kelvin-Helmholtz vortices, we used the formula of τ_{int} based on the mixing length model implemented in the Exchange Discharge Model (EDM) of Bousmar et al. (1999), defined as:

$$\tau_{int} = \rho \psi^t (U_m - U_f)^2 \quad (9)$$

where ψ^t is a turbulent exchange coefficient (in the ISM, ψ^t equals to 0.02 when calibrated from experiments in three different flumes with smooth FPs, see Proust et al. 2009)

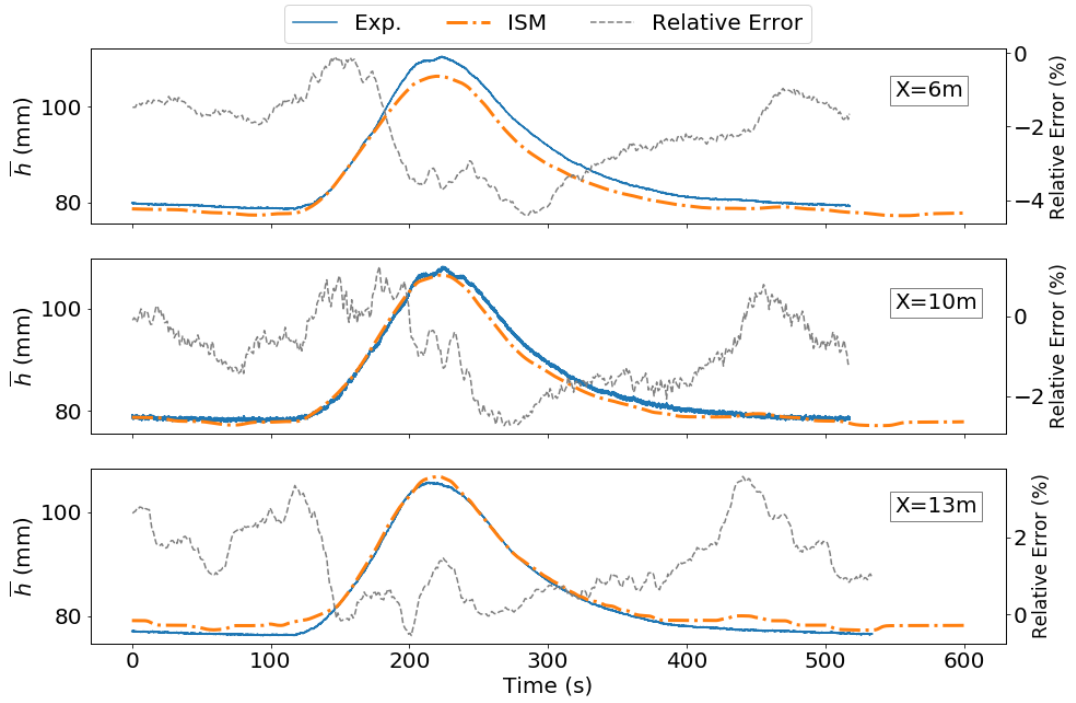

Figure 5: ISM simulation vs. experimental data of the flow depth averaged across the channel $\overline{h}$, and relative error on $\overline{h}$.

5 NUMERICAL VS EXPERIMENTAL RESULTS

At the upstream boundary (X = 0 m), the ISM simulations account for the measured inlet discharge hydrographs in MC and FP. At the downstream boundary , we consider the stage hydrograph measured at X = 15 m. Comparisons between experimental and numerical results were carried out for (1) the flow depth at various X-positions; and (2) depth-averaged streamwise and transverse velocities, lateral

discharge and depth-averaged Reynolds shear stress (not shown here) at the MC-FP interface at X = 10 m. The relative error between numerical result and measurement is calculated as follows:

$$\mathrm{RE_P}\ (\mathrm{t}) = \frac{\mathrm{P_{simulated}(t)} - < \mathrm{P_{measured}} > (\mathrm{t})}{< \mathrm{P_{measured}} > (\mathrm{t})} \tag{10}$$

5.1 Stage hydrographs

For comparing computed and measured flow depths, we used the flow depth averaged across the compound channel, denoted as $\overline{h}$ and defined as:

$$\bar{h} = \frac{A_m + A_f}{B_m + B_f} \tag{11}$$

where B_m and B_f are the widths of MC and FP, respectively. Flow depth $\overline{h}$ is shown in Figure 5. The relative error on $\overline{h}$ is in the range –3% to 5% between X = 6 m and 14 m.

Figure 6 shows that the simulation of flow depth is not sensitive to the turbulent exchange coefficient ψ^t (in Eq. 9, the Reynolds shear stress increases with the ψ^t –values modifying the energy gain/loss in a sub-section, Eqs. 5-6). The same result holds when modifying the weighting coefficient Φ in the formula of the interfacial velocity (Eq. 8).

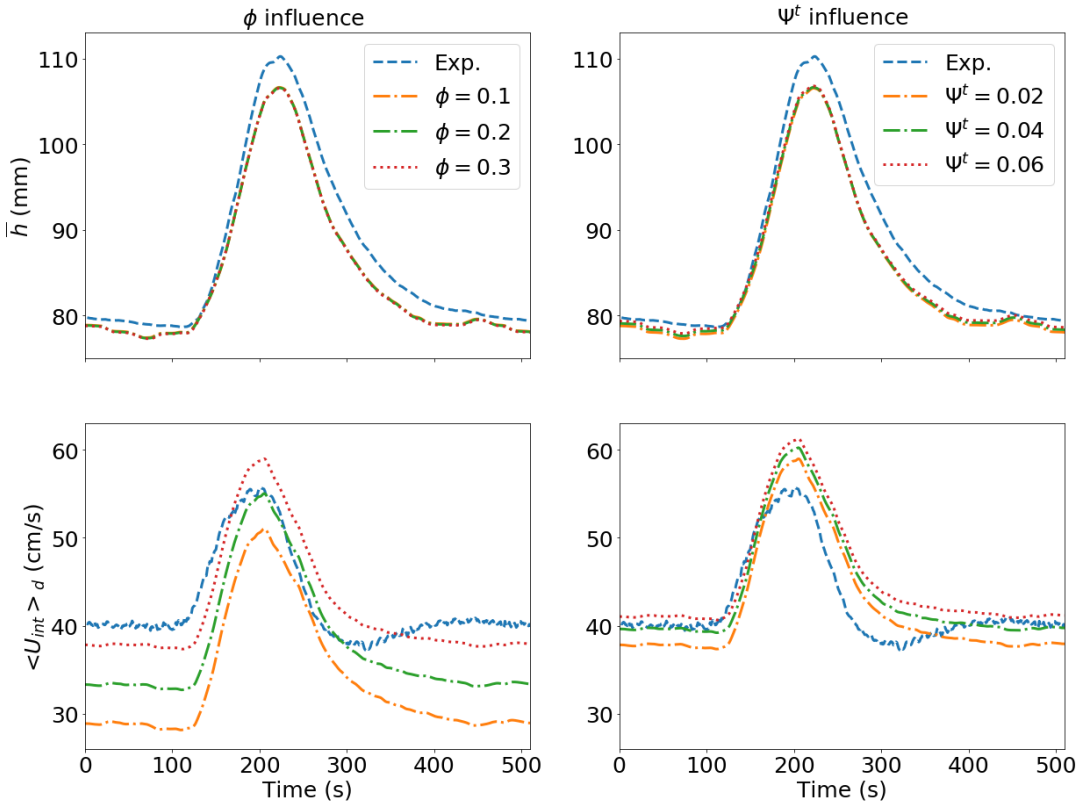

Figure 6: Influence of the weighting coefficient Φ (first column) and of the turbulent exchange coefficient ψ^t on the simulation of flow depth $\overline{h}$ and velocity $<U_{int}>_d$ at X = 10 m.

5.2 Interfacial velocity and lateral discharge

The simulated depth-averaged streamwise velocity $<U_{int}>_d$, transverse velocity $<V_{int}>_d$ (=q/h_f), and lateral discharge q (Eq. 7) at the MC/FP interface are shown in Figure 7 (using Φ= 0.3 in Eq. 8 and ψ^t

=0.02 in Eq. 9). The time evolution and the sign of $<V_{int}>_d$ and q are fairly well reproduced by the model. The evolution of $<U_{int}>_d$ is also well captured with a mean relative error of 11.5% (an a maximum error of 14%). Note that, this velocity is slightly dependent on the turbulent exchange coefficient ψ^t and, more importantly on the weighting coefficient Φ (Figure 6).

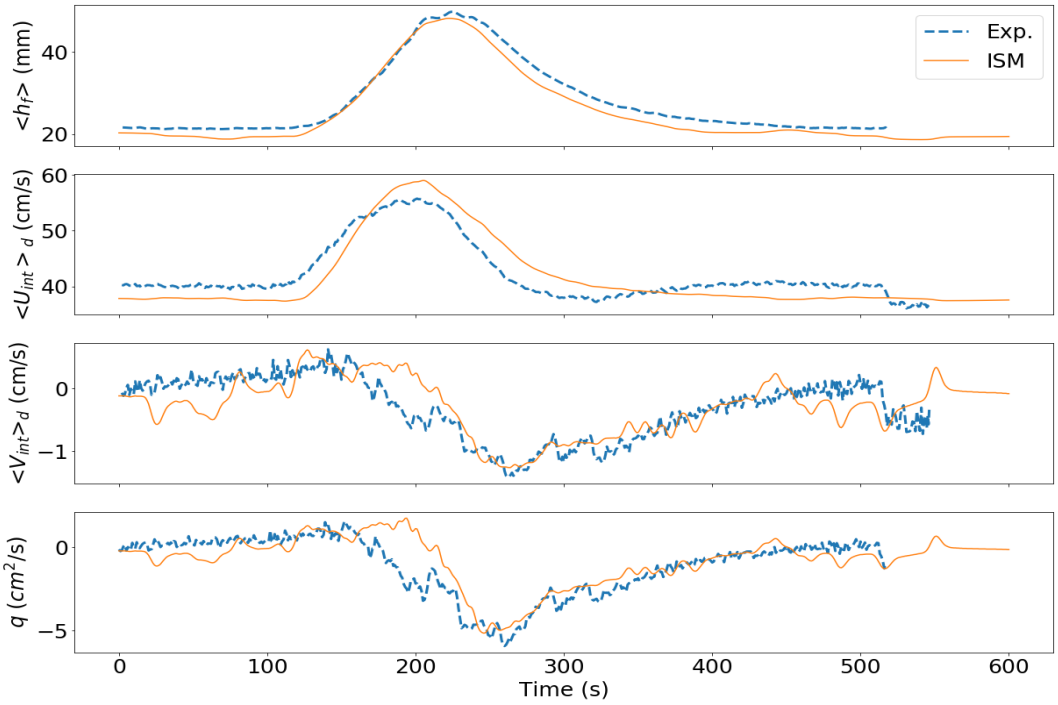

Figure 7: Measured and simulated FP flow depth $<h_f>$, depth-averaged streamwise velocity $<U_{int}>_d$, transverse velocity $<V_{int}>_d$, and lateral discharge q at X = 10 m.

6 CONCLUSION

Unsteady flows were investigated in an asymmetric compound open-channel flume. Hydrographs in the main channel (MC) and floodplain (FP) were injected at the flume entrance, with 100 runs to compute ensemble averages of the flow parameters. The convergence of the total discharge and subsection discharges was obtained for 60 runs, and the convergence of the flow depth for 90 runs. With 100 runs, the interfacial velocity is converged at ±2%. The propagation evolution of the peak flow depth along the flume differs in MC and FP (the peak subsidence is different).

Simulations of these flows using a 1D+ approach (ISM) were performed. The ISM solves the momentum equation in each sub-section (MC and FP), explicitly models the depth-averaged Reynolds stress at the MC/FP interface, and the transverse exchanges of mass and momentum by the mean flow between MC and FP. Last, the ISM account for the measured upstream hydrographs in MC and FP and measured stage hydrograph downstream.

Comparing simulations and experimental data show that the ISM can predict the temporal variations in: (i) the average flow depth across the channel with a relative error ranging from -3% and 5%; and (ii) the depth-averaged streamwise velocity at the MC/FP interface with a relative error of 12%. The temporal evolution and the sign of the depth-averaged transverse velocity and lateral discharge are also well simulated, but relative errors are more significant owing to the low values of the transverse velocities. Last, the temporal dynamics of the flow depth was found to be very little dependent on the transverse exchange of streamwise momentum by the Reynolds shear stress and by the mean flow.

ACKNOWLEDGEMENTS

The authors are grateful to thank Fabien Thollet and Alexis Buffet for their technical support during the experiments. The PhD scholarship of Yasine Kaddi is funded by Irstea (50%) and Compagnie Nationale du Rhône (50%).

Références

Bousmar, Didier, et al. «Uniform flow in prismatic compond channel: Benchmarking numerical models.» *River Flow - Costantinescu, Garcia & Hanes.* 2016. 272-279.

Bousmar, Didier, et Yves Zech. «Momentum transfer for practical flow computation in compound channels.» *J. of Hydrau. Eng.* 125, n° 7 (1999): 696-796.

Bousmar, Didier, N. Wilkin, JH Jacquemart, et Yves Zech. «Overbank flow in symmetrically narrowing floodplains.» *Journal of Hydraulic Engineering* 130, n° 4 (2004): 305-312.

Bousmar, Didier, Sébastien Proust, et Yves Zech. «Experiments on the flow in an enlarging compound channel.» *River Flow 2006: Proceedings of the International Conference on Fluvial Hydraulics.* Lisbon, Portugal: R. M. L. Ferreira et al., 2006. 323 - 332.

Dupuis, Victor, Sébastien Proust, Céline Berni, et André Paquier. «Compound channel flow with a longitudinal transition in hydraulic roughness over the floodplains.» *Environmental Fluid Mechanics* 17, n° 5 (2017b): 903 - 928.

Elliot, S. C. A., et R. H. J. Sellin. «SERC flood channel facility: Skewed flow experiments.» *Journal of Hydraulic Research* 28, n° 2 (1990): 197 - 214.

Knight, D, et K Shiono. «Turbulence measurements in a shear layer region of a compound channel.» *Journal of Hydraulic Research* 28, n° 2 (1990): 175 - 196.

Lai, Chan-Ji, Chang-Ling Liu, et Yeu-Zen Lin. «Experiments on flood-wave propagation in compound channel.» *Journal of Hydraulic Engineering* 126, n° 7 (2000): 492 - 501.

Nicollet, et Uan. «Ecoulements permanents à surface libre en lits composés.» *La Houille Blanche* (La Houille Blanche), 1979: 21 - 30.

Peltier, Yves, Nicolas Rivière, Sébastien Proust, Emmanuel Mignot, André Paquier, et K. Shiono. «Estimation of the error on the mean velocity and on the Reynolds stress due to a misoriented ADV probe in the horizontal plane: Case of experiments in a compound open-channel.» *Flow Meas. Instrum.* 34 (2013b): 34-41.

Peltier, Yves, Sébastien Proust, Nicolas Rivière, André Paquier, et K. Shiono. «Turbulent flows in straight compound open-channel with a transverse embankment on the floodplain.» *J. Hydraul. Res.* 51, n° 4 (2013a): 446- 458.

Proust , Sébastien, Nicolas Rivière, Didier Bousmar, André Paquier, et R. Morel. «Flow in compound channel with abrupt floodplain contraction.» *Journal of Hydraulic Engineering* 132, n° 9 (2006a): 958 - 970.

Proust, Sébastien, Didier Bousmar, Nicolas Rivière, André Paquier, et Yves Zech. «Energy losses in compound open channels.» *Adv. Water Resour.* 33 (2010): 1-16.

Proust, Sébastien, Didier Bousmar, Nicolas Rivière, André Paquier, et Yves Zech. «Nonuniform flow in compound channel: a 1D method for assessing water level and discharge distribution.» *Water Resour. Res.* 45 (2009): 1-16.

Proust, Sébastien, et Vladimir Nikora. «Flow structure in compound open-channel flows in the presence of transverse currents.» *River Flow 2018 - Ninth International Conference on Fluvial Hydraulics.* 2018. 1 - 8.

Proust, Sébastien, J. N. Fernandes, J. B. Leal, Nicolas Rivière, et Yves Peltier. «Mixing layer and coherent structures in compound channel flows: effects of transverse flow, velocity ratio and vertical confinement.» *Water Resources Research*, 2017: 3387 - 3406.

Proust, Sébastien, J. N. Fernandes, Yves Peltier, J.B. Leal, Nicolas Rivière, et A.H. Cardoso. «Turbulent non-uniform flows in straight compound open-channel.» *Journal of Hydraulic Research* 51, n° 6 (2013): 656 - 667.

Sellin, R. H. J. «A Laboratory investigation into the interaction between flow in the channel of a river and that of its floodplain.» *La Houille Blanche*, 1964: 689 - 789.

Takahashi , T. «Theory of one-dimensional unsteady flows in a prismatic open-channel.» *Ann. Dis. Prev. Res. Inst., Kyoto University* 12B (1969): 515-527 (in Japanese).

Tominaga, A., J. Liu, M. Nagao, et I. Nezu. «Hydraulic characteristics of unsteady flow in open channels with flood plains.» *Proceeding of the 26th IAHR congress.* London, 1995. 373 - 378.

Tominaga, Akihiro, M. Nagao, N. Mio, et J. Liu. «Hydraulic characteristics of flood waves passing compound channels.» *Proceedings of hydraulic engineering* 38 (1994): 443 - 448.